Journal of
Experimental
Botany
www.jxb.oxfordjournals.org

RESEARCH PAPER

Threshold response of mesophyll CO_2 conductance to leaf hydraulics in highly transpiring hybrid poplar clones exposed to soil drying

Guillaume Théroux-Rancourt[1], Gilbert Éthier[1] and Steeve Pepin[2,*]

[1] Department of Plant Sciences, Horticultural Research Center, Université Laval, 2480 boul. Hochelaga, Quebec, QC, G1V 0A6, Canada
[2] Department of Soil and Agri-Food Engineering, Horticultural Research Center, Université Laval, 2480 boul. Hochelaga, Quebec, QC, G1V 0A6, Canada

* To whom correspondence should be addressed. E-mail: steeve.pepin@fsaa.ulaval.ca

Abstract

Mesophyll conductance (g_m) has been shown to impose significant limitations to net CO_2 assimilation (A) in various species during water stress. Net CO_2 assimilation is also limited by stomatal conductance to water (g_{sw}), both having been shown to co-vary with leaf hydraulic conductance (K_{leaf}). Lately, several studies have suggested a close functional link between K_{leaf}, g_{sw}, and g_m. However, such relationships could only be circumstantial since a recent study has shown that the response of g_m to drought could merely be an artefactual consequence of a reduced intercellular CO_2 mole fraction (C_i). Experiments were conducted on 8-week-old hybrid poplar cuttings to determine the relationship between K_{leaf}, g_{sw}, and g_m in clones of contrasting drought tolerance. It was hypothesized that changes in g_{sw} and K_{leaf} in response to drought would not impact on g_m over most of its range. The results show that K_{leaf} decreased in concert with g_{sw} as drought proceeded, whereas g_m measured at a normalized C_i remained relatively constant up to a g_{sw} threshold of ~0.15 mol m^{-2} s^{-1}. This delayed g_m response prevented a substantial decline in A at the early stage of the drought, thereby enhancing water use efficiency. Reducing the stomatal limitation of droughted plants by diminishing the ambient CO_2 concentration of the air did not modify g_m or K_{leaf}. The relationship between gas exchange and leaf hydraulics was similar in both drought-tolerant and drought-sensitive clones despite their contrasting vulnerability to stem cavitation and stomatal response to soil drying. The results support the hypothesis of a partial hydraulic isolation of the mesophyll from the main transpiration pathway.

Key words: Drought, internal CO_2 conductance, leaf hydraulic conductance, *Populus*, stomatal limitation, water use efficiency.

Introduction

Attempts to establish significant relationships between physiological variables relating CO_2 assimilation to water transport have been helpful for our understanding of leaf processes under different environmental conditions. For instance, Brodribb and Holbrook (2003, 2004) observed concerted decreases in net photosynthesis (A), stomatal conductance to water (g_{sw}), and leaf hydraulic conductance (K_{leaf}) in tropical tree species during periods of low soil water availability and/or high evaporative demand. These reductions in gas

exchange have been considered a way to avoid major cavitation events by maintaining leaf water potential above a critical threshold (Sack and Holbrook, 2006), a mechanism also observed with stem hydraulic conductance (K_{stem}) (Tyree and Sperry, 1988). Further, there is growing evidence of greater diurnal variation in K_{leaf} than in K_{stem}, which suggests that K_{leaf} is more closely coupled to gas exchange (Brodribb and Holbrook, 2004; Sack and Holbrook 2006). Of the different leaf resistance components, xylem cavitation is the most

important source of resistance to water transport in highly transpiring plants, whereas the resistance occurring outside the xylem represents about a third of the total resistance to leaf water movement (Sack *et al.*, 2004, 2005). Nonetheless, a decline in water transport outside the xylem generally occurs during drought stress due to a shift from the symplastic–transcellular to the apoplastic water pathways, which also produces a decrease in K_{leaf} and g_{sw} (Pou *et al.*, 2013). Thus, in highly vascularized plants such as hybrid poplar, it may be expected that during drought, leaf xylem cavitation would precede an eventual shift of water flow to the outer xylary water pathways. This in turn would lead to a decrease in K_{leaf} and gas exchange as a way to protect the leaf against excessive cavitation.

When considering how environmental conditions may affect CO_2 transport inside leaves, one must take into account the mesophyll conductance (g_m) pertaining to the CO_2 diffusion path from the substomatal cavities to the chloroplast stroma (Ethier and Livingston, 2004; Evans *et al.*, 2009; Tholen *et al.*, 2012). Although an apparent dynamic regulation of g_m in changing microclimates or growth conditions has frequently been reported in recent years (reviewed in Flexas *et al.*, 2008), the physiological basis of such g_m responses and how these changes orchestrate themselves with parallel changes in K_{leaf} and g_{sw} remain poorly understood. For example, g_m and g_{sw} appear to decline in concert as a result of drought stress (Warren, 2008; Centritto *et al.*, 2009; Barbour *et al.*, 2010). However, some studies dealing mainly with short- to mid-term drought stress show little to no relationship between g_m and g_{sw} (Galle *et al.*, 2009; Resco *et al.*, 2009), thereby suggesting a possible threshold drought response of g_m in some species (see, for example, Duan *et al.*, 2011).

Because K_{leaf} is a measure of the ease with which liquid water perfuses through the leaf (Sack and Holbrook, 2006), and since part of this pathway (the mesophyll apoplastic–symplastic–transcellular pathway) is shared with CO_2 diffusing towards the chloroplast as bicarbonate ion and dissolved gas (Kaldenhoff *et al.*, 2008), one would expect a functional linkage between g_m and K_{leaf}, be it in the form of the hydration status of the cell, or even perhaps through convergence of aquaporin-mediated membrane transport (Maurel *et al.*, 2008; Uehlein *et al.*, 2012). Aasamaa *et al.* (2005) showed that K_{leaf} increases with mesophyll density, a trait known to influence g_m (Loreto *et al.*, 1992; Fleck *et al.*, 2010). Moreover, they suggested that membrane-associated traits such as membrane permeability, or simply the frequency of plasmalemmas and tonoplasts in the hydraulic flow path of the mesophyll, were most influential on K_{leaf}. The possibility that membranes also exert strong control over g_m is currently a much debated subject (reviewed in Kaldenhoff, 2012). Recently, Ferrio *et al.* (2012) suggested that the relationship between g_m and K_{leaf} would only be noticeable below a certain threshold. Presumably, the decrease of K_{leaf} and g_m as a result of water stress would be due to an eventual reduction of plasma membrane H_2O/CO_2 permeability, which in turn would divert symplastic water transport through the more tortuous apoplastic pathway (see also Ferrio *et al.*, 2009).

Despite the plausibility of the hypothesis of Ferrio *et al.*, recent modelling results by Tholen *et al.* (2012) offer perhaps a simpler alternative explanation. Indeed, they have theoretically demonstrated that a threshold-like decrease of g_m with respect to g_{sw} in response to drought or salinity stress is expected merely from the relative increase in photorespiratory CO_2 release ensuing from the eventual reduction of the intercellular CO_2 mole fraction (C_i) at low enough g_{sw}. Thus, the apparent threshold-like response of g_m to drought could merely be an artefactual consequence of a reduction of C_i—not a reduction of, say, cell membrane permeability as Ferrio *et al.* (2012) suggested.

To examine possible functional links between K_{leaf}, g_{sw}, and g_m, as well as to verify the possible occurrence of a threshold-like response of g_m with respect to the other two leaf variables, the time course of leaf gas exchange was determined in parallel to K_{leaf} and g_m in hybrid poplars of contrasting drought tolerance during a short-term drought. It was also determined whether a reduction of stomatal limitation via a low CO_2 treatment affects the short-term response of g_m after 1 week of reduced irrigation. To avoid any artefactual CO_2 effects on g_m during measurements, care was taken to conduct the latter under constant C_i. It was hypothesized that g_m, thus evaluated at a normalized C_i, would remain relatively constant and not display a threshold-like response in relation to g_{sw} and K_{leaf}, and that low CO_2 treatment at the end of the drought period would increase g_{sw} in the short term, but not g_m and possibly not K_{leaf}.

Materials and methods

Plant material and growing conditions

Frozen cuttings of Assiniboine [(*Populus*×'Walker':*Populus deltoides* L.×*P.*×*petrowskiana* R.I. Schrod. ex Regel)×male parent unknown] and Okanese [(*P.*×'Walker')×*P.*×*petrowskiana*], with low and high putative drought tolerance, respectively (Silim *et al.*, 2009), were thawed in water for 24 h and sprouted in a mist chamber for ~3 weeks in a 2:1 perlite:Pro-mix growing medium (Premier Horticulture, Rivière-du-Loup, QC, Canada). Plants were transferred to a 2:1 coarse sand:Pro-mix soil in 7 l pots and moved to a greenhouse for ~3 weeks (23/21 °C day/night temperature, 55% relative humidity, 16 h photoperiod). When plants reached ~60 cm in height, they were transferred to a growth cabinet and acclimated for at least 7 d [22/17 °C day/night temperature, 60% relative humidity, 16 h photoperiod, 800 μmol m^{-2} s^{-1} photosynthetic photon flux density (PPFD)]. A 20–20–20 complete nutrient solution was applied twice a week for a total of 200 ppm N per week per plant. Experiments described later were carried out in the same growth cabinet under the same growing conditions.

Gas exchange and fluorescence measurement

Gas exchange measurements were carried out when plants had reached a leaf plastochron index (LPI) of at least 12 (Larson and Isebrands, 1971). Plants were measured between 9:00 h and 12:00 h with a LI-6400XT equipped with a 6400–40 Leaf Chamber Fluorometer (LCF, LI-COR Biosciences, Lincoln, NE, USA). Leaves were initially acclimated under 800 μmol m^{-2} s^{-1} PPFD, 25.0±0.2 °C leaf temperature, 380 μmol mol^{-1} leaf chamber air CO_2 (C_a), 17.5±0.5 mmol mol^{-1} water vapour mole fraction, and 250 μmol s^{-1} air flow rate. Net CO_2 assimilation rate at ambient

conditions ($A_{Ca=380}$), stomatal conductance to water vapour (g_{sw}), and intercellular CO$_2$ mole fraction (C_i) were recorded once gas exchange variables reached steady state. Photochemical efficiency of photosystem II (Φ_{PSII}) was estimated by recording steady-state fluorescence (F_s) and maximal fluorescence under a saturating flash (F_m') of ~10 000 µmol m^{-2} s^{-1} using:

$$\Phi_{PSII} = (F_m' - F_s) / F_m' \tag{1}$$

Mesophyll conductance measurements and calibration

The variable J method (Harley *et al.*, 1992) was used to estimate g_m using:

$$g_m = A / \left\{ C_i - \Gamma^* \times \left[J_f + 8 \left(A + R_d \right) \right] / \left[J_f - 4 \times \left(A + R_d \right) \right] \right\} \tag{2}$$

where J_f is the photochemical electron transport rate estimated from chlorophyll fluorescence, Γ^* is the chloroplastic CO$_2$ photocompensation point, and R_d is the non-photorespiratory mitochondrial respiration in the light, which was estimated from the intersection point of two detailed A–C_i curves performed at 500 and 150 µmol m^{-2} s^{-1} PPFD. For these 'Laisk method' measurements of R_d, a larger 2×3 cm leaf chamber and an air flow rate of 500 µmol s^{-1} were used to minimize chamber leaks (LI-COR, 2012). Since the intersection point of the A–C_i curves of the Laisk method can only give an apparent intercellular CO$_2$ photocompensation point (C_i^*), this value is usually converted to its chloroplastic Γ^* equivalent assuming (von Caemmerer *et al.*, 1994; Ethier and Livingston, 2004):

$$\Gamma^* = C_i^* + R_d / g_m \tag{3}$$

However, this relationship assumes that the great majority of the gross intracellular CO$_2$ flux crossing the chloroplast envelope also experiences the diffusional resistance due to the cell wall and plasmalemma (r_{wp}). As explained in detail in Tholen *et al.* (2012), this is very unlikely, especially around Γ^* where the net outgoing flux R_d crossing the wall/plasmalemma is typically only ~20% of the intracellular flux entering the chloroplast. Under such conditions, Equation 3 may be re-written as:

$$\Gamma^* = C_i^* + R_d \left(r_{wp} - r_{ch} / 0.2 \right) \tag{4}$$

where r_{ch} is the diffusional resistance due to the chloroplast envelope and stroma. Given that current estimates put $r_{ch} \geq r_{wp}$ in non-sclerophylls (Uehlein *et al.*, 2008; Tholen and Zhu, 2011; Tholen *et al.*, 2012), it is clear that C_i^* is probably greater than Γ^*, rather than smaller as Equation 3 has it (see Tholen *et al.*, 2012 for further discussion). Given such uncertainties, it was chosen here to estimate Γ^* in hybrid poplar from previous *in vitro* determinations of the specificity factor ($S_{c/o}$) of Rubisco purified from other woody deciduous species ($S_{c/o}$=100–104; see Balaguer *et al.*, 1996; Bota *et al.*, 2002), which on average corresponded to a Γ^* of ~38 µmol mol^{-1} at 21% O$_2$. This Γ^* value appears in accordance with Equation 4 as it is below the average C_i^* value found here for the poplar clones (40.3 µmol mol^{-1}); it also compares very well with the popular tobacco Γ^* values commonly used to model photosynthesis and estimate g_m (see von Caemmerer *et al.*, 1994; Bernacchi *et al.*, 2002). Furthermore, Galmès *et al.* (2006) have shown the unreliability of *in vivo* Γ^* estimates under water stress conditions, whereas leaf respiration—in particular dark leaf respiration (R_n)—appeared less affected by drought. Consequently, the Laisk method was only used to estimate R_d and establish a relationship with R_n under well-watered conditions, and then this relationship was used to estimate R_d from R_n measurements in all subsequent experiments (see next section).

Calibrations of the relationship between the photochemical electron transport rate estimated from fluorescence measurements (J_f) and gas exchange (J_{CO2}) were carried out as described by Hassiotou *et al.* (2009). Briefly, CO$_2$ response curves were carried out under non-photorespiratory conditions (1% O$_2$) at a PPFD of 1000 µmol m^{-2} s^{-1} by progressively increasing C_a from 300 µmol mol^{-1} up to saturating CO$_2$ (between 800 and 1000 µmol mol^{-1}), which were followed by photosynthetic light responses curves, decreasing PPFD from 1500 to 500 µmol m^{-2} s^{-1} (Fig. 1). This allowed the calculation of J_f as:

$$J_f = [(\Phi_{PSII} \times s) + c] \times PPFD \tag{5}$$

where s is the slope and c the intercept of the relationship of Φ_{PSII} and Φ_{CO2} at 1% O$_2$, Φ_{CO2} being calculated as:

$$\Phi_{CO2} = 4 \times (A + R_d) / PPFD \tag{6}$$

Calibrations carried out on water-stressed plants resulted in similar regressions; hence, data from both well-watered and stressed plants were pooled in the final (Fig. 1).

Nevertheless, such calibration of J_f under non-photorespiratory conditions did not always produce acceptable g_m values (see Gilbert *et al.*, 2012 for a detailed discussion of this issue), as many were negative or too high, particularly when the plants were under water stress. Consequently, an alternative method, in the authors' view more likely to produce more reliable estimates of s under 21% O$_2$, was evaluated. It is based on the premise that at 21% O$_2$, g_m estimates should in theory vary little over a range of C_i values falling around the RuBP-limited A–C_i curve region where Φ_{PSII} is found to be constant (Tholen and Zhu, 2011). It was confirmed that this
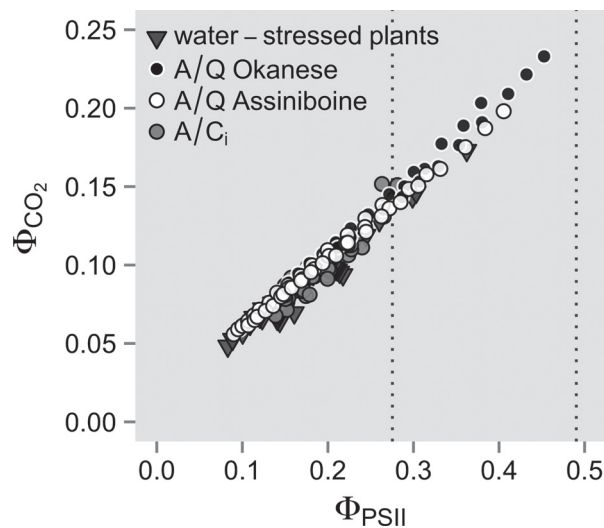
Fig. 1. Relationship between the photochemical electron transport rate estimated from fluorescence measurements (J_f) and gas exchange (J_{CO2}) under 1% O$_2$. Photosynthetic response curves to light (A/Q) and CO$_2$ (A/C_i) were carried out on three plants per clone, and the slope (s) and intercept of the relationship between Φ_{CO2} and Φ_{PSII} were used to calibrate J_f (see Equation 5). A/C_i data were pooled together for clarity. Water-stressed plants were also measured and were in a similar range to well-watered plants. The dotted lines indicate the range of Φ_{PSII} values observed during the short-term soil drying experiments (see Fig. 3). A/Q Okanese, Φ_{CO2}=0.012+0.480×Φ_{PSII}; A/Q Assiniboine, Φ_{CO2}=0.016+0.450×Φ_{PSII}; A/C_i, Φ_{CO2}=0.003+0.496×Φ_{PSII}; water-stressed plants, Φ_{CO2}=0.012+0.433×Φ_{PSII}.

theoretically based assumption held for poplar using g_m measurements obtained with the standard isotopic method of Evans *et al.* (1986) (GE and SP, unpublished; see also Supplementary Fig. S1 available at *JXB* online). Thus, for this alternative J_f calibration method, detailed A–C_i curve analysis around the aforementioned C_i region of interest combined with chlorophyll fluorescence measurements under 21% O_2 was used. s and g_m were then fitted over the C_i range of interest using the RuBP-limited photosynthesis equation given in Ethier *et al.* (2006) (see their equation 3) in order to minimize the sum of squares of errors. This method hence solves s (and so J_f) and g_m simultaneously using the measured A–C_i, Φ_{PSII}, Γ^*, and R_d as inputs.

Net CO_2 assimilation and leaf transpiration rates measured with the LI-6400XT over the aforementioned C_a range were corrected for leaks following the method of Flexas *et al.* (2007a). Briefly, this consisted of subtracting the apparent CO_2 assimilation rate of a dead leaf (immersed in boiling water for 5 min) estimated at the corresponding leaf chamber CO_2 concentration and air flow rate, taking care to allow the leaf to become fully equilibrated with the surrounding water vapour concentration of the chamber (set to 17.5 mmol mol^{-1}). For H_2O leak corrections, the apparent transpiration rate of the empty leaf chamber recorded at 17.5 ± 0.5 mmol mol^{-1} water vapour concentration and appropriate air flow rate was subtracted from measured leaf transpiration rates.

Post-calibration estimation of R_d from dark respiration measurements

Because during the short-term drought experiments the water potential of each leaf used for gas exchange needed to be subsequently rapidly measured with a pressure chamber to determine leaf hydraulic conductance (see 'Leaf hydraulic conductance' below), it was necessary to use a rapid proxy method to estimate R_d immediately following the leaf water potential (Ψ_{leaf}) determination. For this, the leaf petiole was placed in a water-filled beaker and recut under water before clamping the leaf to a LI-6400 equipped with a 2×3 cm leaf chamber, then covering it with a dark cloth to measure its R_n continuously for ~20 min. To convert from R_n to R_d, the following relationship previously established on the plants used for J_f calibrations was used:

$$R_d = 0.4787 R_n \left(n = 12, R^2 = 0.53 \right) \tag{7}$$

Dark respiration was measured at a leaf chamber C_a set equal to the room C_a to avoid CO_2 leakage effects. It was established that pressurization of leaves prior to the determination of dark respiration rates across a range of Ψ_{leaf} (–0.4 to –1 MPa) had no impact on R_n compared with that of unpressurized leaves (data not shown).

Short-term drought

Gas exchange of three plants per clone was repeatedly measured over a 12 d period of soil drying, for a total of nine measuring days. Plants were first measured under well-watered conditions, and the irrigation was then reduced on the following days to achieve a wide range of g_{sw} values. Measurements were carried on the same newly mature leaf (LPI=5 on day 1) throughout the experiment. Soil water potential (Ψ_{soil}) was monitored on each measurement day using custom-made tensiometers and a digital reader (Tensimeter, Soil Moisture Equipment, Santa Barbara, CA, USA).

In addition, to get a better picture of the time course of A, g_{sw}, g_m, and K_{leaf}, continuous measurements of gas exchange and plant and soil water potentials were performed on one plant per clone during 5 d of soil drying. Gas exchange was monitored during daytime with a LI-6400XT equipped with a 2×3 cm adaptor chamber for a PAM-2000 chlorophyll fluorometer probe (Heinz Walz GmbH, Effeltrich, Germany), set at a flash intensity above 6000 µmol m^{-2} s^{-1}. Through Equation 7, R_d was assumed to follow the observed

decreasing trend of R_n as drought proceeded, dropping by ~40–50% after 5 d (from an estimated average initial R_d of ~1.1 µmol m^{-2} s^{-1}). Soil water potential was measured using one tensiometer connected to a datalogger (CR7, Campbell Scientific, Logan, UT, USA). A leaf psychrometer (L-51, Wescor, Logan, UT, USA) was attached on an adjacent leaf to the one used for gas exchange to measure Ψ_{leaf}, while another was attached to an adjacent dark covered leaf to measure Ψ_{stem}. Psychrometer chambers were lightly lined with petroleum jelly to establish a good contact with the leaves (Savage *et al.*, 1983; Campbell and McInnes, 1999). Destructive Ψ_{leaf} and Ψ_{stem} measurements using a pressure chamber were carried out during the time course to correct the psychrometer readings according to a relationship between spot scale (psychrometer) and leaf scale (pressure chamber) water potential measurements established *a priori* (Ψ_{leaf}=1.39 $\Psi_{psychrometer}$, n=96, R^2=0.78; Ψ_{stem}=0.45 $\Psi_{psychrometer}$, n=113, R^2=0.54). To maintain a good contact between the psychrometers and the leaves, the psychrometers were removed daily, inspected, and cleaned if necessary, before resetting them to the leaves. Furthermore, the dark cover for Ψ_{stem} was removed daily after the final gas exchange measurements, ~4–5 h before lights off.

Reduction of drought-induced stomatal limitation using low C_a

Reducing air [CO_2] to very low concentrations around drought- or salt-stressed leaves leads to the opening of stomata to levels that result in a significant reduction of diffusional limitations (Centritto *et al.*, 2003; Bunce, 2007). This technique was thus used on water-stressed leaves to decrease stomatal limitation and monitor changes in A, g_m, and leaf hydraulics.

Prior to soil drying and subsequent low C_a treatment, gas exchange of one leaf (LPI 5–7) was measured under well-watered conditions. Every other day, gas exchange parameters of the same leaf were measured to monitor changes in g_{sw} and to adjust irrigation based on a g_{sw} reduction of ~66% from the well-watered conditions. Soil water content (15 cm TDR probe and Cable tester 1502C, Tektronix, Beaverton, OR, USA) and Ψ_{soil} were monitored daily to adjust irrigation between gas exchange measurements. Well-watered plants were also monitored as comparison.

After 7 d of reduced irrigation, the low C_a treatment was initiated. Gas exchange was measured first under ambient C_a. The plant was then inserted in an ~13 l cylindrical cuvette designed to control the CO_2 and H_2O mole fractions around the plant. Between four and seven leaves, including the previously measured leaf, could be inserted in this large plant cuvette, while the upper and lower parts of the plant (~2–4 leaves each) remained under ambient growth chamber atmosphere (see Supplementary Fig. S2 at *JXB* online for a full description of the cuvette). The target leaf was clamped with the LI-6400XT LCF chamber inside the 13 l plant cuvette and both were sealed. The large plant cuvette operated as an open system, with an inflow of ~12 l min^{-1}. The plant cuvette CO_2 mole fraction was decreased to ~75 µmol mol^{-1} and the H_2O mole fraction was maintained at ~17 mmol mol^{-1} by circulating the cuvette air through a H_2O scrubbing Drierite™ column in series with a CO_2 scrubbing column. A LI-840 CO_2/H_2O Analyzer (LI-COR Biosciences, Lincoln, NE, USA) was used to monitor the plant cuvette gas concentrations. Leaf temperature was maintained at 25 ± 0.2 °C in the leaf chamber. Air temperature in the plant cuvette was ~26 °C, ~1 °C higher than the ambient air temperature outside the cuvette.

After g_{sw} had peaked and stabilized, the CO_2 mole fraction was increased in the leaf chamber to reach a C_i of ~275 µmol mol^{-1} (see chlorophyll fluorescence calibration in the Results section) and C_a in the large plant cuvette was increased in parallel to match the C_a established in the leaf chamber. Once leaf gas exchange had reached steady state, three consecutive measurements were taken, each at least 2 min apart.

Leaf hydraulic conductance

For both the short-term drought and the low C_a experiment, K_{leaf} was estimated using the evaporative flux method:

$$K_{leaf} = E / (\Psi_{stem} - \Psi_{leaf}) \qquad (8)$$

where E is leaf transpiration measured using the LI-6400XT, and Ψ_{stem} (stem water potential; measured on a dark-adapted leaf) and Ψ_{leaf} are measured using a Scholander-type pressure chamber (Model 610, PMS instruments, Albany, OR, USA) or the leaf psychrometers.

Vulnerability curves

Vulnerability curves were carried out using a low-pressure flow meter (LPFM; Sperry *et al.*, 1988). Shoots were cut from plants in the growth chamber, put in a plastic bag, and brought to the lab. After an equilibration period of at least 5 min, water potential was measured on a leaf. Stems were then cut under water, and stem segments of ~7 cm long were prepared based on previous work by Harvey and van den Driessche (1997). Initial stem hydraulic conductivity (K_i) was determined under a pressure head of 4.7 kPa by collecting water flowing out of the segment into a 10 ml pipette and measuring the increasing water column in the pipette with a pressure transducer connected to a datalogger (CR23X, Campbell Scientific). When steady state was reached, stem segments were flushed at a pressure of 120 kPa for 7 min to remove emboli before measuring maximum hydraulic conductivity (K_{max}). Both flushes and conductivity measurements were carried out using a KCl (0.1 M) solution filtered at 0.2 µm (Cai and Tyree, 2010). To reach more negative Ψ_{stem} values, shoots were left to dry in the lab and stem segments were measured upon reaching a desired value. Percentage loss conductivity (PLC) was calculated as:

$$PLC = 100 \times (K_{max} - K_i) / K_{max} \qquad (9)$$

The vulnerability curves were constructed by plotting PLC against Ψ_{stem}, and then fitting a Weibull function:

$$PLC / 100 = 1 - \exp\left[-(-\Psi_{stem} / b)^c\right] \qquad (10)$$

where b and c are fitting constants. Fitting was carried out using the *nls* function in R 3.0.0 (R Core Team, 2013).

Statistical analysis

Statistical analyses were carried out with R 3.0.0. Mixed models were used to determine the hierarchical structure (i.e. plants within a measurement cycle) using the *nlme* procedure (Pinheiro *et al.*, 2013). Initial rates of leaf gas exchange were compared between clones to examine clonal differences. For the low C_a experiment, final measurements were analysed using a two-level factorial design (clone×low C_a treatment).

Results

Calibration of the chlorophyll fluorescence method for estimating the photochemical electron transport rates

Estimates of g_m based on the calibration of J_f under 1% O$_2$ exhibited a positively skewed shape when plotted against C_i, with a narrow maximum at ~200 µmol mol^{-1} (Fig. 2). However, using the proposed alternative calibration method at 21% O$_2$, g_m estimates increased slightly and were more stable for several hundreds of ppm above a C_i of 200 µmol mol^{-1} (Fig. 2). Thus, in order to improve the estimates of g_m as C_i decreases under soil drying conditions, C_a was adjusted in the
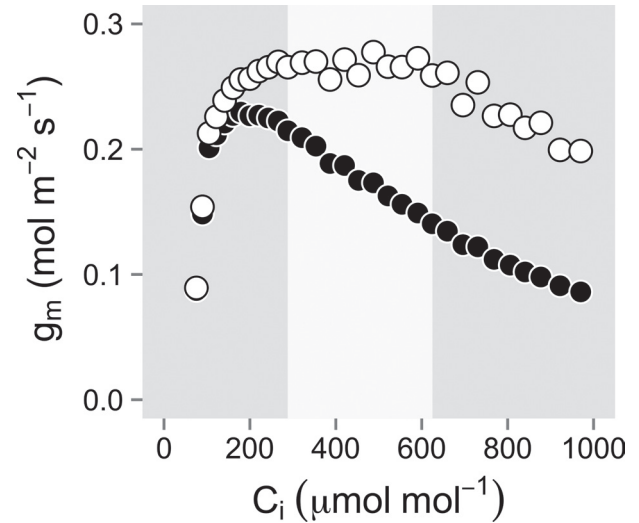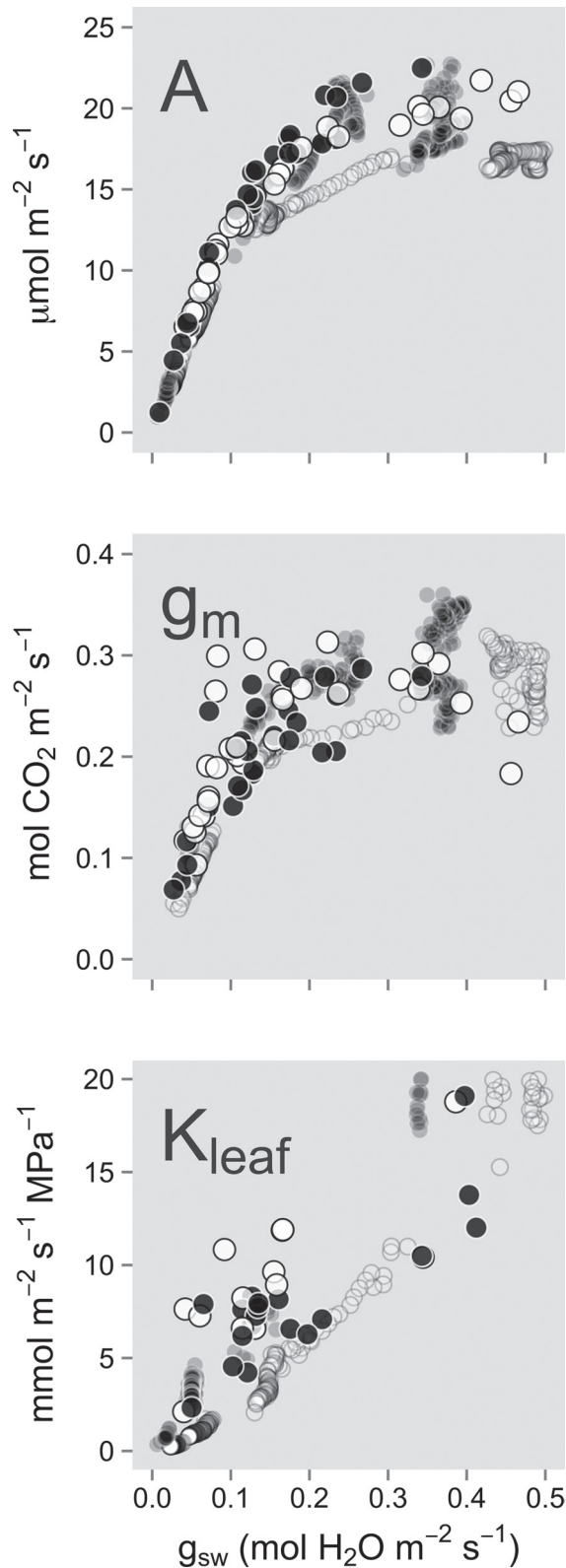

Fig. 2. Apparent response of mesophyll conductance (g_m) to intercellular CO$_2$ mole fraction (C_i) using the 1% O$_2$ calibration method (filled circles) and the proposed 21% O$_2$ A/C_i calibration method (open circles) on one Okanese leaf. The light coloured area represents the RuBP-limited range where Φ_{PSII} is found to be constant. Estimates of s under 1% and 21% O$_2$ were 0.4799 and 0.4572, respectively.
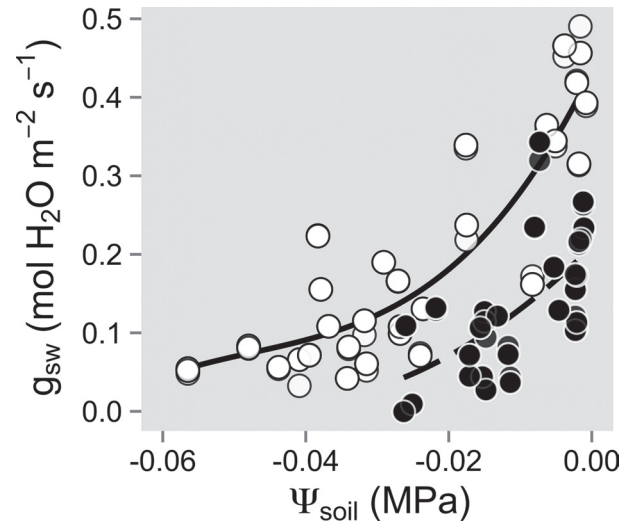
leaf chamber to reach a normalized C_i of 275 µmol mol^{-1} (hereafter named C_i=275), a value consistently identified as the minimal C_i required to reach a stable and maximal g_m. Using a normalized C_i value resulted in <5% of g_m estimates being discarded (i.e. negative or too high values) compared with 15% when measuring at ambient C_a (380 µmol mol^{-1}). Overall, there was a slight difference in s values between clones (see Fig. 1) and the proposed calibration method yielded s estimates that were ~5% lower than those found under 1% O$_2$ (Fig. 2).

Gas exchange responses to short-term drought

Drought-sensitive Assiniboine and drought-tolerant Okanese had, under well-watered conditions, a similar photosynthesis rate under ambient C_a ($A_{Ca=380}$; $F_{1,17}$=2.11, P=0.16), and a similar normalized $g_{m\_Ci=275}$ ($F_{1,16}$=2.93, P=0.11), although g_{sw} was slightly higher in Assiniboine ($F_{1,17}$=3.62, P=0.07; Fig. 3). Twelve days of reduced irrigation gradually decreased photosynthesis ($A_{Ca=380}$), g_{sw}, transpiration (E), K_{leaf}, and leaf and soil water potential (Ψ_{leaf} and Ψ_{soil}) to very low values (e.g. a 90% decrease in g_{sw}; see Figs 3 and 4). The decline in Ψ_{leaf}, E, and K_{leaf} was concomitant with g_{sw}, while the decline in A lagged behind K_{leaf}. Normalized $g_{m\_Ci=275}$ remained constant over most of the drought-induced g_{sw} range, and decreased only when g_{sw} fell below a threshold of ~0.15 mol m^{-2} s^{-1} (i.e. 68% and 56% of the maximum g_{sw} for Assiniboine and Okanese, respectively). However, because too low or near zero g_{sw} led to difficult if not impossible g_m fits, $g_{m\_Ci=275}$ values below 0.05 mol m^{-2} s^{-1} were not included in the analysis as scatter increased

Fig. 4. Responses of stomatal conductance (g_{sw}) to decreasing soil water potential (Ψ_{soil}) during the short-term drought experiment. A second-order polynomial curve was fitted for each clone [Assiniboine (open circles), R^2=0.79; and Okanese (filled circles), R^2=0.39; $P < 0.0001$].

tremendously below that threshold, even using the proposed calibration method.

Although the drought response of $A_{Ca=380}$, K_{leaf}, and $g_{m\_Ci=275}$ appeared similar for both clones when plotted against g_{sw}, for any given Ψ_{soil}, g_{sw} of Okanese was always lower than that of Assiniboine. Hence, for Okanese, the minimal g_{sw} was observed at a Ψ_{soil} of –0.03 MPa, compared with –0.06 MPa for Assiniboine (Fig. 4). Assiniboine reached higher g_{sw} values under well-watered conditions, but this did not translate into an increase in $A_{Ca=380}$, and both clones exhibited a similar decline in $A_{Ca=380}$ at common g_{sw}. Similar gas exchange versus leaf hydraulic relationships to the 12 d reduced irrigation experiment were obtained over 5 d of water depletion during which $A_{Ca=380}$, g_{sw}, K_{leaf}, and g_m (C_i=225–275 µmol mol^{-1}) were recorded continuously. Once again, g_{sw} and K_{leaf} decreased in concert, the decline in $A_{Ca=380}$ lagged behind the two previous variables, and g_m remained constant up to a g_{sw} threshold of ~0.15 mol m^{-2} s^{-1} (Fig. 3; see also Supplementary Fig. S3 at *JXB* online).

Lowering C$_a$ to decrease drought-induced stomatal limitation

After 7 d of reduced irrigation, g_{sw} was decreased by 75% on average in Assiniboine and 69% in Okanese. In both clones, lowering C_a around leaves resulted in a 3- to 4-fold increase in g_{sw} and E, which translated into a significantly more negative Ψ_{leaf} (Table 1). When C_a was reduced, g_{sw} reached a new steady state within 20–40 min for water-stressed plants, and after 50–75 min in well-watered plants (Fig. 5). Furthermore, g_{sw} rapidly declined after a return to a higher C_a in severely stressed plants (white dots in Fig. 5), while well-watered plants showed a more progressive return towards their initial g_{sw} level. In contrast to g_{sw} and Ψ_{leaf}, no significant changes in K_{leaf}, $A_{Ci=275}$, and $g_{m\_Ci=275}$ were observed under low C_a. There were no clonal differences in gas exchange responses

Fig. 3. Changes in photosynthesis (*A*), mesophyll conductance (g_m), and leaf hydraulic conductance (K_{leaf}) in relation to stomatal conductance to water (g_{sw}) during a short-term, moderate water stress. Three plants per clone were measured over 12 d of reduced irrigation, using the same leaf per plant. Assiniboine (drought sensitive; open circles), Okanese (drought tolerant; filled circles). Data from a separate 5 day soil drying experiment are also shown (translucent circles; one plant per clone; same colour code).

Table 1. *Effect of low air CO$_2$ concentration around leaves on gas exchange and leaf hydraulics of water-stressed [foliar transpiration (E) <3 mmol m^{-2} s^{-1}] hybrid poplar clones contrasting in drought tolerance*

Clone (drought tolerance)	C_a	$A_{Ci=275}$ (μmol m^{-2} s^{-1})[a]	$g_{m\_Ci=275}$ (mol m^{-2} s^{-1})	g_{sw} (mol m^{-2} s^{-1})	E (mmol m^{-2} s^{-1})	K_{leaf} (mmol m^{-2} s^{-1} MPa^{-1})	Ψ_{leaf} (MPa)
Okanese	Ambient	18.7 (2.4)[b]	0.224 (0.042)	0.115 (0.053)	1.65 (0.63)	6.43 (2.1)	−0.87 (0.07)
(tolerant)	Low	20.9 (2.4)	0.270 (0.036)	0.325 (0.053)	4.08 (0.63)	9.28 (2.0)	−0.97 (0.07)
Assiniboine	Ambient	21.7 (2.3)	0.285 (0.037)	0.119 (0.051)	1.64 (0.59)	12.2 (2.2)	−0.76 (0.07)
(sensitive)	Low	15.0 (2.6)	0.204 (0.040)	0.206 (0.058)	3.07 (0.68)	14.5 (2.9)	−1.06 (0.08)
P-values[c]	Clone	0.69	0.96	0.22	0.34	0.04	0.66
	C_a	0.35	0.59	0.007	0.007	0.21	0.01
	Clone×C_a	0.06	0.10	0.23	0.44	0.90	0.21

[a] Photosynthesis ($A_{Ci=275}$) and mesophyll conductance ($g_{m\_Ci=275}$) measured at a normalized C_i of 275 μmol mol^{-1}, stomatal conductance to water (g_{sw}), transpiration (E), leaf hydraulic conductance (K_{leaf}), and leaf water potential (Ψ_{leaf}).

[b] Standard error in parentheses.

[c] Numerator d.f. = 1; denominator d.f. = 20 ($A_{Ci=275}$, g_{sw}, Ψ_{leaf}, E), 17 ($g_{m\_Ci=275}$), 11 (K_{leaf}).
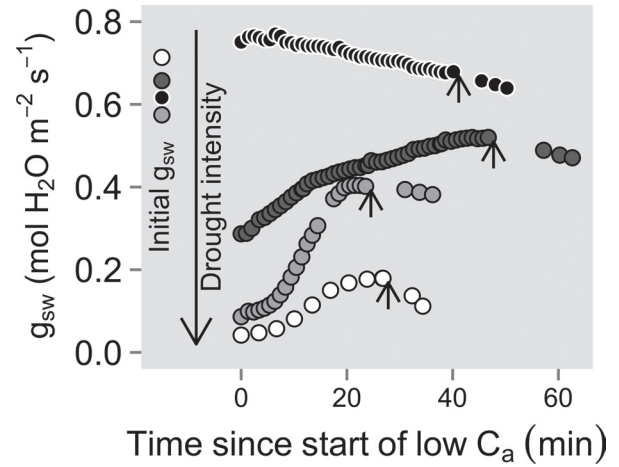
Fig. 5. Time courses of stomatal conductance (g_{sw}) when the upper foliage of well-watered and water-stressed Assiniboine plants was exposed to a reduction in ambient CO$_2$ concentration (C_a ~75 μmol mol^{-1}). Different levels of water stress were examined, expressed here as the percentage of g_{sw} relative to their initial well-watered state (g_{sw_ini}) evaluated 7 d prior to the low C_a treatment (black circles, well-watered, where g_{sw} increased compared with g_{sw_ini}; dark grey circles, 44% of g_{sw_ini}; light grey circles, 15% of g_{sw_ini}; and white circles, 6% of g_{sw_ini}). The short arrows indicate when C_a was increased from ~75 μmol mol^{-1} to a CO$_2$ concentration resulting in a C_i of ~275 μmol mol^{-1}. The data points to the right of the arrows were measured at that C_i, showing the high sensitivity of severely stressed plants to the return to near ambient C_a.

to low CO$_2$ treatment under reduced irrigation, although Assiniboine exhibited higher K_{leaf} than Okanese (Table 1).
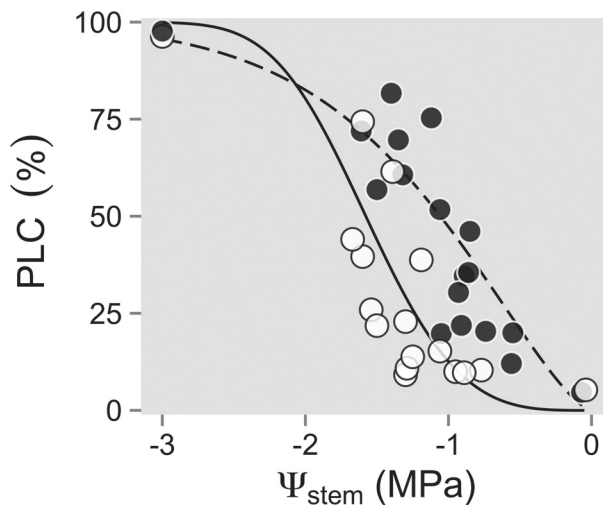
Vulnerability curves

Since each clone exhibited a similar A versus g_{sw} response to drought, as well as a similar response to low C_a exposure, vulnerability to cavitation was measured to determine further the clonal differences in water stress response. Drought-tolerant Okanese exhibited a higher reduction in K_{stem} over the observed Ψ_{stem} range compared with Assiniboine (Fig. 6). For instance, the PLC was up to 50% in Okanese upon reaching a Ψ_{stem} of –1 MPa, while Assiniboine had ~15% PLC at the same potential. However, PLC increased rapidly after –1.2 MPa Ψ_{stem} in Assiniboine to reach similar PLC values to Okanese near –1.5 MPa (Fig. 6). Nevertheless, values of Ψ_{leaf} observed throughout the experiment were on average between –0.6 MPa and –0.9 MPa (first and third quartiles) for both clones, and Ψ_{stem} ranged between –0.3 MPa and –0.6 MPa. Thus, both clones usually did not reach a PLC of 50% but suffered only ~25% loss of conductivity under the moderate drought conditions of this study.

Discussion

Methodological considerations on the estimation of g$_m$

Potential methodological errors and the underlying assumptions necessary in the estimation of g_m using the variable

J method were discussed initially by Harley *et al.* (1992), and subsequently elaborated upon by several other authors (e.g. Warren 2008; Pons *et al.*, 2009; Gilbert *et al.*, 2012). Theoretically, positively skewed g_m versus C_i curves like those observed in this study when following the standard 1% O_2 J_f calibration protocol (see also Flexas *et al.*, 2007b; Hassiotou *et al.*, 2009; Gilbert *et al.*, 2012) are predicted to result from small overestimations of J_f, and/or possibly from underestimations of Γ^*, or of R_d (see Harley *et al.*, 1992; Gilbert *et al.*, 2012). However, Tholen *et al.* (2012) demonstrated that even if all relevant parameters in the variable J method equation were exact, g_m would still be expected to decrease apparently sharply when the photorespiratory CO_2 flux rises at low C_i. One way to alleviate this artefactual CO_2 sensitivity problem is by measuring g_m at a normalized C_i, preferably around the g_m versus C_i curve region where g_m is expected to peak (i.e. the narrow C_i range where estimates of g_m are expected to be least affected by small errors of J_f, etc.; see Fig. 2). However, even after taking this precaution, it was noted that ~5% of the initial g_m estimates for leaves subjected to water stress were deemed unreliable. One possibility that could explain this poor model performance is that the 1% O_2 calibration method incompletely accounts for alternative electron sinks under 21% O_2; especially under water stress (Makino *et al.*, 2002; Kitao *et al.*, 2003; Laisk *et al.*, 2006). In an attempt to address this possibility, we tested an alternative J_f calibration method performed under 21% O_2, and which solves s and g_m concurrently from the CO_2 response of photosynthesis and Φ_{PSII} in the RuBP-limited A–C_i curve region where photorespiration is expected to be low enough to exert little influence on g_m (see Fig. 2, and further details in the Materials and methods). From the present assessment, this alternative J_f calibration procedure yielded slightly lower photochemical electron transport rates than the 1% O_2 calibration method, which resulted in ~20% higher g_m estimates, but did not improve the rejection of data under water stress conditions. Nevertheless, it is believed that calibrating Φ_{CO2} under 21%

O_2 should better account for potential alternative electron sinks under normal atmospheric conditions while greatly simplifying the calibration procedure.

To evaluate possible g_m inaccuracies introduced by errors in the estimation of Γ^* and R_d, an analysis of the sensitivity of g_m to changes in Γ^* (±10%) and R_d (±50%) was performed. As already pointed out by others (e.g. Harley *et al.*, 1992; Pons *et al.*, 2009), g_m was significantly more sensitive to potential errors in Γ^* in comparison with R_d (see Fig. 7)—in the present simulations, a 120% increase in R_d was necessary to obtain a g_m value corresponding to a +10% change in Γ^*. However, because the estimation of g_m was restricted to a narrow C_i range neighbouring 275 µmol mol^{-1}, such errors in Γ^* and/or R_d are not expected to change the conclusions regarding the delayed threshold response of g_m with respect to g_{sw} (see Fig. 7).

Threshold response of g$_m$ to drought

Drought stress usually decreases A, g_{sw}, and K_{leaf} concomitantly (Brodribb and Holbrook, 2006; Brodribb *et al.*, 2007; Warren, 2008; Galle *et al.*, 2009; Barbour *et al.*, 2010). Drought stress has also been shown to decrease g_m monotonically with respect to A and g_{sw} (Flexas *et al.*, 2007b, 2008; Warren, 2008; Perez-Martin *et al.*, 2009), although Flexas *et al.* (2002) reported a lower rate of g_m decrease at g_{sw} >0.15 mol H$_2$O m^{-2} s^{-1} in grapevine. However, these declines in g_m may only be circumstantial since a recent study has shown that g_m is expected to decrease apparently sharply in the absence of any change in intraleaf diffusional resistance component, once the photorespiratory rate of a water-stressed leaf rises significantly due to stomatal closure and ensuing reduction in C_i (Tholen *et al.*, 2012). Measuring g_m at
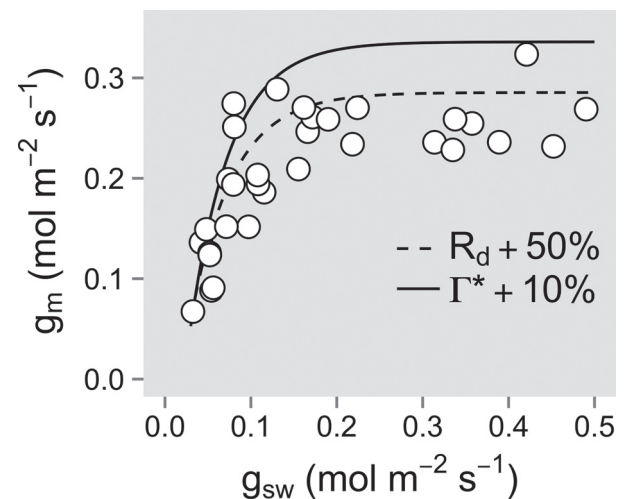

Fig. 6. Stem vulnerability curve to cavitation (PLC: percentage loss conductivity) in drought-tolerant Okanese (filled circles) and drought-sensitive Assiniboine (open circles) hybrid poplar clones.

Fig. 7. Sensitivity of mesophyll conductance (g_m) estimates to a 10% increase in chloroplastic CO_2 photocompensation point (Γ*, solid line) or a 50% increase in non-photorespiratory mitochondrial respiration in the light (R_d, dashed line). Asymptotic fits of the simulated data were used to represent the observed variations. Data from Assiniboine in Fig. 3 were used (original data: open circles).

a normalized C_i alleviates this effect, which allowed detection of a threshold response of g_m with respect to g_{sw} (~0.15 mol H_2O m^{-2} s^{-1}), thereby confirming the observations of Ferrio *et al.* (2012). This recent study demonstrated a strong linear relationship between g_m and K_{lamina} (hydraulic conductance of the leaf lamina), but only when K_{lamina} fell below 8 mmol H_2O m^{-2} s^{-1} MPa^{-1} (~70% of maximum value) as a result of water stress. Above this threshold point, corresponding to g_m values ≥0.2 mol m^{-2} s^{-1}, the relationship did not hold, as the effective water path length influencing K_{lamina} reached a constant baseline value. Hence, the g_m–K_{lamina} sensitivity region corresponded to the point where the water path length between the xylem and the evaporative surface increased significantly above this baseline value.

The small difference in g_m threshold between the study of Ferrio *et al*. and the present study could arise from the different species and their respective hydraulic connectivity, but also because a constant C_i was used for g_m measurement with the variable J method (Harley *et al.*, 1992). Using a normalized C_i improved g_m estimates, as they reached similar values between clones. Nonetheless, in both studies, g_{sw} responded rapidly to early signs of water stress, and g_m followed afterwards. Concomitantly, Φ_{PSII}, although not an ideal proxy for g_m, has shown a delay in decrease as Ψ_{leaf} declined, beginning its descent often past a g_{sw} reduction of 50% or even 80% (Brodribb and Holbrook, 2003), as observed in the present study (Fig. 3). Hydraulic compartmentalization of the mesophyll might have contributed to this delayed response of g_m. Two factors are important when considering compartmentalization: the linkage between the xylem and the epidermis, and the degree of uncoupling of the mesophyll cell to the hydraulic apparatus (Zwieniecki *et al.*, 2007). Thus, stomata, sensing early signs of water stress through small changes in Ψ_{leaf}, could have started to close while more negative Ψ_{leaf} values (i.e. more severe stress) may have been needed to initiate a response in mesophyll cells or chloroplasts, leading to a decrease in g_m. Zwieniecki *et al.* (2007) explained that such hydraulic compartmentalization would allow mesophyll cells to be buffered against short-term changes in leaf water status, a beneficial characteristic to C-assimilating cells. Also, the bulk of mesophyll cells have been shown to be rather unresponsive to exogeneously applied abscisic acid (ABA) (Shatil-Cohen *et al.*, 2011), which reinforces the idea that mesophyll cells are somewhat isolated from the main hydraulic path linking the xylem conduits and their bundle sheath extensions to the epidermis and stomata. Such structural considerations may act in conjunction with membrane-associated mechanisms such as gating of aquaporin channels and ensuing reduction of the symplastic water transport (Cochard *et al.*, 2007; Almeida-Rodriguez *et al.*, 2010; Pou *et al.*, 2013), which might eventually divert more water to the more tortuous apoplastic pathway (Ferrio *et al.*, 2012). The above model appears to fit well the hydraulic response of the hybrid poplar leaves despite the fact that it makes little mention of xylem cavitation. Certainly, the present results show that Ψ_{stem} did not reach low enough values to induce substantial stem cavitation (see also Secchi and Zwieniecki, 2010), but this does not necessarily mean that significant leaf cavitation could not have occurred. Indeed, Sack *et al.* (2004, 2005) reported that the xylem-related component of total leaf resistance dominates in highly transpiring plants such as hybrid poplar, and recently Johnson *et al.* (2012) demonstrated that in some species leaf xylem cavitation may account for most of the decrease in K_{leaf} under drought.

Exposure to low C_a decouples g_s and g_m

Centritto *et al.* (2003) proposed a method to separate diffusional limitations from non-diffusional limitations in salt-stressed plants: they lowered C_a to force stomata to open, thus reducing stomatal limitation upon returning to ambient C_a. Surprisingly, the low C_a treatment appeared to reduce the mesophyll limitation just as rapidly as the stomatal limitation. However, the C_i values at which Centritto *et al.* (2003) evaluated g_m after pre-conditioning the stressed plants to low C_a was appreciably higher than before the low C_a treatment. Thus, because g_m was not evaluated at a normalized C_i in this study, it is likely that the conclusions of Centritto *et al.* (2003) about the rapid response of g_m to salt stress were confounded by the low C_i photorespiratory artefacts described in Tholen *et al.* (2012). In the present case, C_i was controlled close to 275 µmol mol^{-1} throughout and no significant change in g_m in response to low C_a pre-conditioning was detected.

Apart from its obvious consequences on gas exchange, low C_a treatment has major consequences for the leaf water status. As in the present study, Bunce (2007) reported a decrease (more negative) in Ψ_{leaf} using low C_a on a variety of water-stressed herbaceous and woody plants. Interestingly, the hybrid poplar plants used here reached a common Ψ_{leaf} value (approximately –0.92 MPa to –1.01 MPa) under low C_a regardless of drought intensity, which suggests that the degree of stomatal opening could have been modulated to keep Ψ_{leaf} above a catastrophic cavitation level (see also the results of Tardieu and Simonneau, 1998). If leaf xylem cavitation and concomitant decrease in Ψ_{leaf} were responsible for the decline in K_{leaf} under drought, K_{leaf} would have been expected to decrease more as a result of the low C_a treatment since Ψ_{leaf} was further reduced (see Table 1 compared with Supplementary Fig. S4 at *JXB* online). However, it did not, and similar observations by Bunce (2007) led him to question the dominant role of leaf cavitation in drought-induced K_{leaf} decline. One recent alternative explanation is a possible dual regulation of g_{sw} and K_{leaf} by ABA under soil drying conditions (Pantin *et al.*, 2013). Indeed, in the present study, water-stressed plants exhibited greater stomatal sensitivity to changes in C_a than well-watered plants (Fig. 5), a trait normally associated with the presence of higher levels of ABA (Raschke, 1975; Bunce, 2007).

Cochard *et al.* (2007) reported that aquaporin expression in the leaf vein bundle sheaths could be a major control point on leaf water status, observing a substantial drop in Ψ_{leaf} when aquaporin activity was inhibited. Shatil-Cohen *et al.* (2011) have also shown that either drought or exogenous application of ABA triggered a reduction of the permeability coefficient (and thus K_{leaf}) of bundle sheath cells, but not that of the mesophyll cells. As previously

mentioned, this suggests a partial hydraulic isolation of mesophyll cells from the xylem–bundle sheath–stomata pathway, thereby possibly delaying ABA delivery. Since certain aquaporins have been reported to have a CO_2 channel role (Otto *et al.*, 2010; Uehlein *et al.*, 2012), it may be that g_m is less sensitive to drought stress than g_{sw} or K_{leaf} because regulation of mesophyll aquaporins is expected to take place at a more advanced drought stress due to hydraulic compartmentalization.

Delayed g_m *response to drought favours water use efficiency in hybrid poplar*

One aim of the present study was to compare two clones of contrasting drought tolerance in order to determine if they differ in their g_{sw}, K_{leaf}, and g_m relationships. Both drought-tolerant Okanese and drought-sensitive Assiniboine exhibited a similar g_m threshold response to drought (Fig. 3), potentially suggesting a partial hydraulic isolation of the mesophyll cells. This in turn allowed a delay in the decline of *A*, thereby favouring a higher water use efficiency (WUE) during the early stages of drought. However, those clones differed in their vulnerability to stem cavitation and in the Ψ_{soil} at which their respective minimal g_{sw} was reached (Fig. 4), as observed in other hybrid poplar studies (Silim *et al.*, 2009; Arango-Velez *et al.*, 2011; Larcheveque *et al.*, 2011). Although the vulnerability curves in the present study showed that Okanese allowed more cavitation to occur at similar Ψ_{stem} values than Assiniboine (Fig. 6), both clones modulated g_{sw} to maintain Ψ_{stem} at levels preventing conductivity to drop below ~25%, a feature previously observed for those same clones under severe drought stress (Arango-Velez *et al.*, 2011). While Okanese maintained similar $A_{Ca=380}$ and g_m to Assiniboine at a given g_{sw}, it adopted a more conservative water use strategy by lowering g_{sw} more than Assiniboine under increasing soil water depletion (see also Arango-Velez *et al.*, 2011). Hence, Okanese exhibited a higher intrinsic water use efficiency (WUE_i) than Assiniboine at comparable Ψ_{soil} (it also displayed a higher g_m/g_{sw} ratio; data not shown). Such maintenance of high g_m/g_{sw} ratios has recently been identified as an important trait to improve WUE in cultivated plants (Barbour *et al.*, 2010; Flexas *et al.*, 2013).

Conclusion

When subjecting young hybrid poplar clones of contrasting drought tolerance to a short period of water stress, K_{leaf} and g_{sw} decreased monotonically in concert, while g_m remained constant over most of its range, causing a delay in the decline of *A*. Only when g_{sw} fell below an approximate threshold of 0.15 mol m^{-2} s^{-1}, ~33% (Assiniboine) to 40% (Okanese) of maximum g_{sw}, was a decrease in g_m observed (and this even when measured at a normalized C_i to remove the photorespiratory bias modelled by Tholen *et al.*, 2012), in accordance with the recent results of Ferrio *et al.* (2012). The present results thus support the recent suggestion that the bulk mesophyll is partially isolated (i.e. buffered) from the major transpiration pathway delivering ABA to the stomata (Shatil-Cohen *et al.*, 2011; Pantin *et al.*, 2013). The delayed photosynthetic decline mediated by such a g_m threshold response resulted in enhancing WUE in the early stage of drought.

Supplementary data

Supplementary data are available at *JXB* online.

Figure S1. Apparent sensitivity of mesophyll conductance (g_m) to intercellular CO_2 mole fraction (C_i): comparison of the responses observed under three different g_m estimation methods.

Figure S2. Schematic of the large plant cuvette used in the low C_a experiment.

Figure S3. Continuous measurements of photosynthesis (*A*), mesophyll conductance (g_m), stomatal conductance to water (g_{sw}), and leaf hydraulic conductance (K_{leaf}) during 5 d of water depletion.

Figure S4. Relationship between leaf hydraulic conductance (K_{leaf}) and leaf water potential (Ψ_{leaf}) during 5 d of water depletion.

Acknowledgements

References

Aasamaa K, Niinemets U, Sober A. 2005. Leaf hydraulic conductance in relation to anatomical and functional traits during *Populus tremula* leaf ontogeny. *Tree Physiology* **25,** 1409–1418.

Almeida-Rodriguez AM, Cooke JE, Yeh F, Zwiazek JJ. 2010. Functional characterization of drought-responsive aquaporins in *Populus balsamifera* and *Populus simonii×balsamifera* clones with different drought resistance strategies. *Physiologia Plantarum* **140,** 321–333.

Arango-Velez A, Zwiazek JJ, Thomas BR, Tyree MT. 2011. Stomatal factors and vulnerability of stem xylem to cavitation in poplars. *Physiologia Plantarum* **143,** 154–165.

Balaguer L, Affi D, Dizengremel P, Dreyer E. 1996. Specificity factor of ribulose bisphosphate carboxylase/oxygenase of *Quercus robur*. *Plant Physiology and Biochemistry* **34,** 879–883.

Barbour MM, Warren CR, Farquhar GD, Forrester G, Brown H. 2010. Variability in mesophyll conductance between barley genotypes, and effects on transpiration efficiency and carbon isotope discrimination. *Plant, Cell and Environment* **33,** 1176–1185.

Bernacchi CJ, Portis AR, Nakano H, von Caemmerer S, Long SP. 2002. Temperature response of mesophyll conductance.

Implications for the determination of Rubisco enzyme kinetics and for limitations to photosynthesis *in vivo*. *Plant Physiology* **130,** 1992–1998.

Bota J, Flexas J, Keys AJ, Loveland J, Parry MAJ, Medrano H. 2002. CO_2/O_2 specificity factor of ribulose-1,5-bisphosphate carboxylase/oxygenase in grapevines (*Vitis vinifera* L.): first *in vitro* determination and comparison to *in vivo* estimations. *Vitis* **41,** 163–168.

Brodribb TJ, Feild TS, Jordan GJ. 2007. Leaf maximum photosynthetic rate and venation are linked by hydraulics. *Plant Physiology* **144,** 1890–1898.

Brodribb TJ, Holbrook NM. 2003. Stomatal closure during leaf dehydration, correlation with other leaf physiological traits. *Plant Physiology* **132,** 2166–2173.

Brodribb TJ, Holbrook NM. 2004. Diurnal depression of leaf hydraulic conductance in a tropical tree species. *Plant, Cell and Environment* **27,** 820–827.

Brodribb TJ, Holbrook NM. 2006. Declining hydraulic efficiency as transpiring leaves desiccate: two types of response. *Plant, Cell and Environment* **29,** 2205–2215.

Bunce JA. 2007. Low carbon dioxide concentrations can reverse stomatal closure during water stress. *Physiologia Plantarum* **130,** 552–559.

Cai J, Tyree MT. 2010. The impact of vessel size on vulnerability curves: data and models for within-species variability in saplings of aspen, *Populus tremuloides* Michx. *Plant, Cell and Environment* **33,** 1059–1069.

Campbell CS, McInnes KJ. 1999. Response of *in situ* leaf psychrometer to cuticle removal by abrasion. *Agronomy Journal* **91,** 859–862.

Centritto M, Lauteri M, Monteverdi MC, Serraj R. 2009. Leaf gas exchange, carbon isotope discrimination, and grain yield in contrasting rice genotypes subjected to water deficits during the reproductive stage. *Journal of Experimental Botany* **60,** 2325–2339.

Centritto M, Loreto F, Chartzoulakis K. 2003. The use of low [CO_2] to estimate diffusional and non-diffusional limitations of photosynthetic capacity of salt-stressed olive saplings. *Plant, Cell and Environment* **26,** 585–594.

Cochard H, Venisse JS, Barigah TS, Brunel N, Herbette S, Guilliot A, Tyree MT, Sakr S. 2007. Putative role of aquaporins in variable hydraulic conductance of leaves in response to light. *Plant Physiology* **143,** 122–133.

Duan B, Ran F, Zhang X, Zhang. Y. 2011. Long-term acclimation of mesophyll conductance, carbon isotope discrimination and growth in two contrasting *Picea asperata* populations exposed to drought and enhanced UV-B radiation for three years. *Agricultural and Forest Meteorology* **151,** 116–126.

Ethier GJ, Livingston NJ. 2004. On the need to incorporate sensitivity to CO_2 transfer conductance into the Farquhar–von Caemmerer–Berry leaf photosynthesis model. *Plant, Cell and Environment* **27,** 137–153.

Ethier GJ, Livingston NJ, Harrison DL, Black TA, Moran JA. 2006. Low stomatal and internal conductance to CO_2 versus Rubisco deactivation as determinants of the photosynthetic decline of ageing evergreen leaves. *Plant, Cell and Environment* **29,** 2168–2184.

Evans JR, Kaldenhoff R, Genty B, Terashima I. 2009. Resistances along the CO_2 diffusion pathway inside leaves. *Journal of Experimental Botany* **60,** 2235–2248.

Evans JR, Sharkey TD, Berry JA, Farquhar GD. 1986. Carbon isotope discrimination measured concurrently with gas exchange to investigate CO_2 diffusion in leaves of higher plants. *Australian Journal of Plant Physiology* **13,** 281–292.

Ferrio JP, Cuntz M, Offermann C, Siegwolf R, Saurer M, Gessler A. 2009. Effect of water availability on leaf water isotopic enrichment in beech seedlings shows limitations of current fractionation models. *Plant, Cell and Environment* **32,** 1285–1296.

Ferrio JP, Pou A, Florez-Sarasa I, Gessler A, Kodama N, Flexas J, Ribas-Carbo M. 2012. The Peclet effect on leaf water enrichment correlates with leaf hydraulic conductance and mesophyll conductance for CO_2. *Plant, Cell and Environment* **35,** 611–625.

Fleck I, Peña-Rojas K, Aranda X. 2010. Mesophyll conductance to CO_2 and leaf morphological characteristics under drought stress during *Quercus ilex* L. resprouting. *Annals of Forest Science* **67,** 308–308.

Flexas J, Bota J, Escalona JM, Sampol B, Medrano H. 2002. Effects of drought on photosynthesis in grapevines under field conditions: an evaluation of stomatal and mesophyll limitations. *Functional Plant Biology* **29,** 461–471.

Flexas J, Diaz-Espejo A, Berry J A, Cifre J, Galmes J, Kaldenhoff R, Medrano H, Ribas-Carbo M. 2007a. Analysis of leakage in IRGA's leaf chambers of open gas exchange systems: quantification and its effects in photosynthesis parameterization. *Journal of Experimental Botany* **58,** 1533–1543.

Flexas J, Diaz-Espejo A, Galmes J, Kaldenhoff R, Medrano H, Ribas-Carbo M. 2007b. Rapid variations of mesophyll conductance in response to changes in CO_2 concentration around leaves. *Plant, Cell and Environment* **30,** 1284–1298.

Flexas J, Niinemets U, Galle A, *et al*. 2013. Diffusional conductances to CO_2 as a target for increasing photosynthesis and photosynthetic water-use efficiency. *Photosynthesis Research* . **117,** 45–59.

Flexas J, Ribas-Carbo M, Diaz-Espejo A, Galmes J, Medrano H. 2008. Mesophyll conductance to CO_2: current knowledge and future prospects. *Plant, Cell and Environment* **31,** 602–621.

Galle A, Florez-Sarasa I, Tomas M, Pou A, Medrano H, Ribas-Carbo M, Flexas J. 2009. The role of mesophyll conductance during water stress and recovery in tobacco (*Nicotiana sylvestris*): acclimation or limitation? *Journal of Experimental Botany* **60,** 2407–2418.

Galmès J, Medrano H, Flexas J. 2006. Acclimation of Rubisco specificity factor to drought in tobacco: discrepancies between *in vitro* and *in vivo* estimations. *Journal of Experimental Botany* **57,** 3659–3667.

Gilbert ME, Pou A, Zwieniecki MA, Holbrook NM. 2012. On measuring the response of mesophyll conductance to carbon dioxide with the variable J method. *Journal of Experimental Botany* **63,** 413–425.

Harley PC, Loreto F, Di M, Giorgio, Sharkey TD. 1992. Theoretical considerations when estimating the mesophyll conductance to CO_2 flux by analysis of the response of photosynthesis to CO_2. *Plant Physiology* **98,** 1429–1436.

Harvey HP, van den Driessche R. 1997. Nutrition, xylem cavitation and drought resistance in hybrid poplar. *Tree Physiology* **17,** 647–654.

Hassiotou F, Ludwig M, Renton M, Veneklaas EJ, Evans JR. 2009. Influence of leaf dry mass per area, CO_2, and irradiance on mesophyll conductance in sclerophylls. *Journal of Experimental Botany* **60,** 2303–2314.

Johnson DM, McCulloh KA, Woodruff DR, Meinzer FC. 2012. Evidence for xylem embolism as a primary factor in dehydration-induced declines in leaf hydraulic conductance. *Plant, Cell and Environment* **35,** 760–769.

Kaldenhoff R. 2012. Mechanisms underlying CO_2 diffusion in leaves. *Current Opinion in Plant Biology* **15,** 276–281.

Kaldenhoff R, Ribas-Carbo M, Sans JF, Lovisolo C, Heckwolf M, Uehlein N. 2008. Aquaporins and plant water balance. *Plant, Cell and Environment* **31,** 658–666.

Kitao M, Lei TT, Koike T, Tobita H, Maruyama Y. 2003. Higher electron transport rate observed at low intercellular CO_2 concentration in long-term drought-acclimated leaves of Japanese mountain birch (*Betula ermanii*). *Physiologia Plantarum* **118,** 406–413.

Laisk A, Eichelmann H, Oja V, Rasulov B, Ramma H. 2006. Photosystem II cycle and alternative electron flow in leaves. *Plant and Cell Physiology* **47,** 972–983.

Larcheveque M, Maurel M, Desrochers A, Larocque GR. 2011. How does drought tolerance compare between two improved hybrids of balsam poplar and an unimproved native species? *Tree Physiology* **31,** 240–249.

Larson PR, Isebrands JG. 1971. The plastochron index as applied to developmental studies of cottonwood. *Canadian Journal of Forest Research* **1,** 1–11.

LI-COR Biosciences. 2012. *LI-6400 XT user manual* . Lincoln, NE: LI-COR Biosciences.

Loreto F, Harley PC, Di Marco G and Sharkey TD. 1992. Estimation of mesophyll conductance to CO_2 flux by three different methods. *Plant Physiology* **98,** 1437–1443.

Makino A, Miyake C, Yokota A. 2002. Physiological functions of the water–water cycle (Mehler reaction) and the cyclic electron flow around PSI in rice leaves. *Plant and Cell Physiology* **43,** 1017–1026.

Maurel C, Verdoucq L, Luu DT, Santoni V. 2008. Plant aquaporins: membrane channels with multiple integrated functions. *Annual Review of Plant Biology* **59,** 595–624.

Otto B, Uehlein N, Sdorra S, *et al*. 2010. Aquaporin tetramer composition modifies the function of tobacco aquaporins. *Journal of Biological Chemistry* **285,** 31253–31260.

Pantin F, Monnet F, Jannaud D, Costa JM, Renaud J, Muller B, Simonneau T, Genty B. 2013. The dual effect of abscisic acid on stomata. *New Phytologist* **197,** 65–72.

Perez-Martin A, Flexas J, Ribas-Carbo M, Bota J, Tomas M, Infante JM, Diaz-Espejo A. 2009. Interactive effects of soil water deficit and air vapour pressure deficit on mesophyll conductance to CO_2 in *Vitis vinifera* and *Olea europaea*. *Journal of Experimental Botany* **60,** 2391–2405.

Pinheiro J, Bates D, DebRoy S, Sarkar D, R Core Team. 2013. *nlme: linear and nonlinear mixed effects models*. R package version 3.1–109.

Pons TL, Flexas J, von Caemmerer S, Evans JR, Genty B, Ribas-Carbo M, Brugnoli E. 2009. Estimating mesophyll conductance to CO_2: methodology, potential errors, and recommendations. *Journal of Experimental Botany* **60,** 2217–2234.

Pou A, Medrano H, Flexas J, Tyerman SD. 2013. A putative role for TIP and PIP aquaporins in dynamics of leaf hydraulic and stomatal conductances in grapevine under water stress and re-watering. *Plant, Cell and Environment* **36,** 828–843.

Raschke K. 1975. Simultaneous requirement of carbon dioxide and abscisic acid for stomatal closing in *Xanthium strumarium* L. *Planta* **125,** 243–259.

R Core Team. 2013. *R: a language and environment for statistical computing*. R Foundation for Statistical Computing, Vienna, Austria. http://www.R-project.org/.

Resco V, Ewers BE, Sun W, Huxman TE, Weltzin JF, Williams DG. 2009. Drought-induced hydraulic limitations constrain leaf gas exchange recovery after precipitation pulses in the C3 woody legume, *Prosopis velutina*. *New Phytologist* **181,** 672–682.

Sack L, Holbrook NM. 2006. Leaf hydraulics. *Annual Review of Plant Biology* **57,** 361–381.

Sack L, Streeter CM, Holbrook NM. 2004. Hydraulic analysis of water flow through leaves of sugar maple and red oak. *Plant Physiology* **134,** 1824–1833.

Sack L, Tyree MT, Holbrook NM. 2005. Leaf hydraulic architecture correlates with regeneration irradiance in tropical rainforest trees. *New Phytologist* **167,** 403–413.

Savage MJ, Wiebe HH, Cass A. 1983. *In situ* field measurement of leaf water potential using thermocouple psychrometers. *Plant Physiology* **73,** 609–613.

Secchi F, Zwieniecki MA. 2010. Patterns of PIP gene expression in *Populus trichocarpa* during recovery from xylem embolism suggest a major role for the PIP1 aquaporin subfamily as moderators of refilling process. *Plant, Cell and Environment* **33,** 1285–1297.

Shatil-Cohen A, Attia Z, Moshelion M. 2011. Bundle-sheath cell regulation of xylem–mesophyll water transport via aquaporins under drought stress: a target of xylem-borne ABA? *The Plant Journal* **67,** 72–80.

Silim S, Nash R, Reynard D, White B, Schroeder W. 2009. Leaf gas exchange and water potential responses to drought in nine poplar (*Populus* spp.) clones with contrasting drought tolerance. *Trees-Structure and Function* **23,** 959–969.

Sperry JS, Donnelly JR, Tyree MT. 1988. A method for measuring hydraulic conductivity and embolism in xylem. *Plant, Cell and Environment* **11,** 35–40.

Tardieu F, Simonneau T. 1998. Variability among species of stomatal control under fluctuating soil water status and evaporative demand: modelling isohydric and anisohydric behaviours. *Journal of Experimental Botany* **49,** 419–432.

Tholen D, Ethier G, Genty B, Pepin S, Zhu XG. 2012. Variable mesophyll conductance revisited: theoretical background and experimental implications. *Plant, Cell and Environment* **35,** 2087–2103.

Tholen D, Zhu XG. 2011. The mechanistic basis of internal conductance: a theoretical analysis of mesophyll cell photosynthesis and CO_2 diffusion. *Plant Physiology* **156,** 90–105.

Tyree MT, Sperry JS. 1988. Do woody plants operate near the point of catastrophic xylem dysfunction caused by dynamic water stress? Answers from a model. *Plant Physiology* **88,** 574–580.

Uehlein N, Otto B, Hanson DT, Fischer M, McDowell N, Kaldenhoff R. 2008. Function of *Nicotiana tabacum* aquaporins as chloroplast gas pores challenges the concept of membrane CO$_2$ permeability. *The Plant Cell* **20,** 648–657.

Uehlein N, Sperling H, Heckwolf M, Kaldenhoff R. 2012. The Arabidopsis aquaporin PIP1;2 rules cellular CO$_2$ uptake. *Plant, Cell and Environment* **35,** 1077–1083.

von Caemmerer S, Evans JR, Hudson GS, Andrews TJ. 1994. The kinetics of ribulose-1,5-bisphosphate carboxylase/oxygenase *in vivo* inferred from measurements of photosynthesis in leaves of transgenic tobacco. *Planta* **195,** 88–97.

Warren CR. 2008. Soil water deficits decrease the internal conductance to CO$_2$ transfer but atmospheric water deficits do not. *Journal of Experimental Botany* **59,** 327–334.

Zwieniecki MA, Brodribb TJ, Holbrook NM. 2007. Hydraulic design of leaves: insights from rehydration kinetics. *Plant, Cell and Environment* **30,** 910–921.